Classical and quantum routes to linear magnetoresistance

JINGSHI HU AND T. F. ROSENBAUM*

The James Franck Institute and Department of Physics, The University of Chicago, Chicago, Illinois 60637, USA

*e-mail: tfr@uchicago.edu

Published online: 24 August 2008; doi:10.1038/nmat2259

The hallmark of materials science is the ability to tailor the microstructure of a given material to provide a desired response. Carbon mixed with iron provides the steel of buildings and bridges; impurities sprinkled in silicon single crystals form the raw materials of the electronics revolution; pinning centres in superconductors let them become powerful magnets. Here, we show that either adding a few parts per million of the proper chemical impurities to indium antimonide, a well-known semiconductor, or redesigning the material's structure on the micrometre scale, can transform its response to an applied magnetic field. The former approach is purely quantum mechanical[1–3]; the latter a classical outgrowth of disorder[4–7], turned to advantage. In both cases, the magnetoresistive response—at the heart of magnetic sensor technology—can be converted to a simple, large and linear function of field that does not saturate. Harnessing the effects of disorder has the further advantage of extending the useful applications range of such a magnetic sensor to very high temperatures by circumventing the usual limitations imposed by phonon scattering.

Symmetry conditions demand a quadratic dependence of the electrical resistivity ρ on magnetic field H in the low-field limit. Semiclassically, the strong-field magnetoresistance saturates quickly to constant value C (ref. 8):

$$\frac{\Delta\rho}{\rho} \propto \begin{cases} (\mu H)^2, & \mu H < 1 \\ C, & \mu H > 1, \end{cases} \qquad (1)$$

where μ is the carriers' mobility. A number of innovative techniques have been used to amplify the magnetoresistance, including spin valves at heterojunctions ('giant' magnetoresistance)[9,10], magnetic-field-driven metal–insulator transitions[11,12] and geometrical inclusions[13]. Sufficiently strong disorder, where current paths no longer align with the applied voltage, can also mix the components of the resistivity tensor in such a way as to escape the strictures of equation (1) (refs 4–7,14), whether or not the material has an intrinsic physical magnetoresistance. A key design feature of this new regime is that the magnitude of the magnetoresistance is no longer controlled by the carrier mobility, but rather by the distribution of mobilities, with the biggest response occurring near band crossing where $\mu \to 0$ and both positive and negative mobilities can be sampled.

Quantum effects become noticeable when the individual quantum levels associated with the electron orbits are distinct: $\hbar\omega_c \gg k_B T$, where ω_c is the cyclotron frequency and T is the temperature. At still higher magnetic fields, it is possible to reach the 'extreme quantum limit', where $\hbar\omega_c$ can exceed the Fermi energy, E_F, and electrons can coalesce into the lowest quantum state of the transverse motion in H. A generic quantum description of galvanomagnetic phenomena was developed by Abrikosov[1–3], with:

$$\rho_{xx} = \rho_{yy} = \frac{N_i H}{\pi n^2 e c} \propto H, \qquad (2)$$

where ρ_{xx} and ρ_{yy} are the transverse components of the magnetoresistance, n is the density of electrons and N_i is the concentration of static scattering centres. This quantum magnetoresistance is linear down to very small fields, positive and non-saturating. However, the necessity of reaching the extreme quantum limit makes practical realizations unique to semi-metals[15,16] and to semiconductors having tiny pockets of the Fermi surface with a small effective mass.

InSb is one such possibility: a narrow-gap semiconductor with unusual electronic properties that result from the low carrier concentration required for metallicity, small conduction electron effective mass, large Fermi wavelength and extremely long carrier mean free path[17]. High-quality single crystals grown both epitaxially and from melt have been used for fundamental studies and in applications such as magnetic-field-sensing devices[18]. Most investigations have focused on heavily doped and compensated samples with multiple carrier species. The resulting magnetotransport involves two types of hole[19,20] and the complications of impurity-band conduction[21]. Deviations from the semiclassical theory (quadratic behaviour and saturation) were observed in n-type InSb at liquid-nitrogen temperature by Frederikse and Hosler[22], but the transverse magnetoresistance still follows a superlinear field dependence and only up to 2.2 T.

In contrast, we can access Abrikosov's quantum linear magnetoresistance by lightly doping single-crystal InSb in such a way that only one carrier type dominates. The specimen contains merely 10^{-5} conduction electrons per unit cell, yet its resistivity is only 50 times that of copper, an indication of its usually large relaxation time (the low-field Hall mobility, $\mu_H = 2.2\,m^2\,V^{-1}\,s^{-1}$ at $T = 300$ K). The extreme quantum limit ($\hbar\omega_c > E_F$) can then be reached at a moderate magnetic field of $H = 2$ T. We compare in Fig. 1 the temperature dependence of the zero-field resistance and the carrier concentration derived from measurements of the Hall effect, assuming a one-band model. Between $T = 30$ and 175 K, all of the impurity donors are thermally activated, leading to a metallic conductivity with extrinsic carrier concentration independent of temperature ($n = N_D = 5 \times 10^{17}\,cm^{-3}$). At higher temperature, the intrinsic carrier concentration n_i becomes larger than N_D, and the resistivity decreases exponentially with

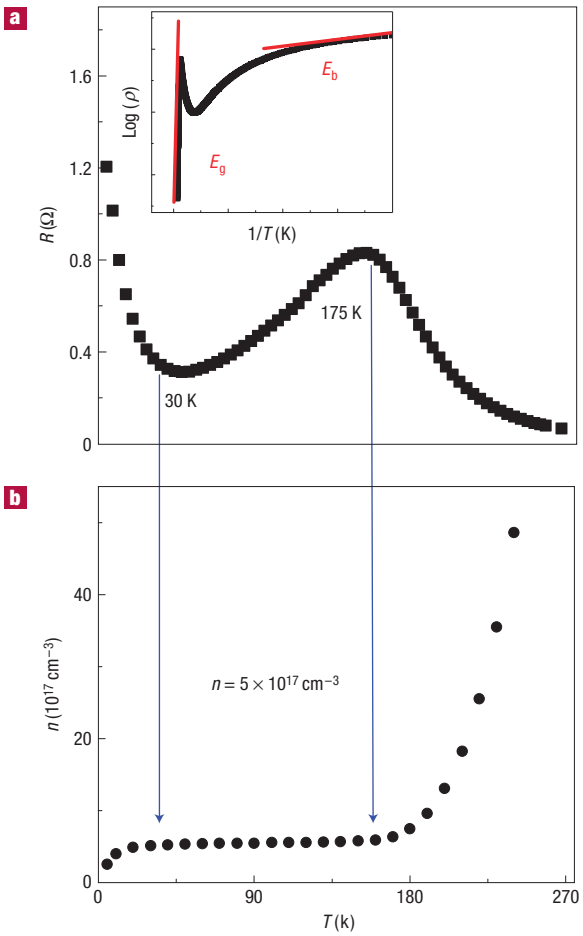

Figure 1 Doping InSb into the quantum regime. a, In the extrinsic region of constant carrier concentration, 30 K < T < 175 K, the resistivity decreases with decreasing temperature owing to decreased phonon scattering. Inset: Activated behaviour dominates the resistivity at temperatures above and below the extrinsic regime. **b**, Variation of carrier concentration with temperature deduced from Hall effect measurements. The n-type donors are Bi and Pb, as confirmed by mass spectroscopy.

temperature in accordance with the usual behaviour of intrinsic semiconductors, $\rho(T) \propto \exp(E_g/2kT)$, with the bandgap energy $E_g = 200$ meV (Fig. 1, inset). As the donors freeze out below 30 K, the resistivity again exhibits an exponential dependence on T, $\rho(T) \propto \exp(E_b/2kT)$, but with a shallower slope than that at high temperatures because the n-type donors Pb and Bi have binding energies $E_b = 0.6\,\text{meV} \ll E_g$.

The regime of extrinsic conductivity, shown as the plateau in Fig. 1a, is characterized by a constant number of degenerate electrons with a quadratic, isotropic dispersion relation and a small effective mass of $0.01m_0$ (m_0 being the free-electron mass). This yields a large Dingle temperature, $T_D = 200$ K, for $H = 2$ T ($\hbar\omega_c \gg k_B T$), and the quantum linear magnetoresistance emerges. Figure 2a shows the positive, linear magnetic field dependence of the transverse magnetoresistance. The size of the effect is huge, exceeding 40,000% by $H = 13$ T at $T = 50$ K. Of particular interest is the temperature dependence of the linear response, which decreases only by a factor of 2 (still of order 20,000% at $H = 13$ T) as the temperature varies from 50 to 175 K. This relative insensitivity to T demonstrates that the magnitude of the linear magnetoresistance is not due to the appearance of phonon scattering, which should lead to a marked decrease with increasing T, but is most likely associated with the concentration of scattering centres, N_i. This behaviour is qualitatively confirmed by the theoretical expression given in equation (2).

The explicit quantum nature of the response can be discerned from the observation of an oscillatory magnetic field response in the low-field magnetoresistance. This effect, known as Shubnikov–de Haas oscillations, indicates the modulated density of states at the Fermi surface as a quantized Landau-level sweeps through the Fermi energy. Figure 2b shows Shubnikov–de Haas oscillations for our crystal of doped InSb. A longitudinal configuration is required to observe the oscillatory behaviour because the background magnetoresistance in a longitudinal field is approximately 10^4 times smaller than its transverse counterpart. The observed oscillations provide clear evidence of Landau quantization over the entire temperature range of the quantum linear magnetoresistance (30–175 K). The peaks (filled circles) and valleys (open circles) of the oscillations scale as expected with $1/H$, with all of the conduction electrons in the lowest Landau level for $H > 2$ T (Fig. 2b, inset). Surprisingly, the crossover from quadratic to linear dependence on magnetic field at $H = 0.7$ T is considerably lower than the predicted value from the condition $\hbar\omega_c > E_F$, pointing to an early emergence of the linear magnetoresistance when not strictly only the lowest, but two or three quantized levels are involved (Fig. 2d). As demonstrated in Fig. 2c, the quadratic magnetic field dependence of the magnetoresistance re-emerges in the intrinsic regime above $T = 200$ K when holes compensate the conduction and the Landau levels smear out rapidly from both thermal and collision broadening. At lower temperatures, the quantum effect breaks down for $T < 10$ K because the electrons freeze out and the semiconductor becomes non-degenerate. With high-level control over the impurity doping levels, sensors with substantially enhanced quantum linear magnetoresistance over an even greater temperature range can readily be anticipated.

Of particular interest for technological applications is the magnetoresistance at and above room temperature. The classical, orbital magnetoresistance above 200 K (Fig. 2c) is controlled by the dimensionless parameter involving the product of the carriers' mobility and magnetic field, $\omega_c\tau = \mu H$, where the cyclotron and effective masses are equal for the simple, parabolic band structure of n-type InSb. Under usual circumstances, the magnitude of the magnetoresistance diminishes rapidly with increased phonon scattering at higher temperatures and the sensitivity diminishes rapidly in all conventional devices. However, it is possible to engineer an exception to this limitation by tapping the benefits of disorder. When gross inhomogeneities exist in a semiconductor—whether or not the material has an intrinsic, physical magnetoresistance—it is possible to create distorted current paths misaligned with the driving voltage, and mix in the off-diagonal components of the magnetoresistivity tensor. As a result, the associated magnetotransport is dominated by the magnitude of the fluctuations in the mobility, $\Delta\mu$, rather than the mobility μ itself. This picture has been used by Parish and Littlewood[4,5], and later the current authors[6,7], to demonstrate that the purely classical, geometric effects of micrometre-long nanowires of excess Ag could be responsible for the non-saturating, linear magnetoresistance in $Ag_{2\pm\delta}Se$ and $Ag_{2\pm\delta}Te$ (refs 23–26).

To this end, we have taken undoped InSb single crystals, ground them into nanopowders, and formed polycrystals with a typical grain size of 10 μm (Fig. 3b, inset), incorporating droplets of single-phased Sb along the grain boundaries as inhomogeneities. InSb is a promising candidate for a robust, responsive, high-temperature magnetoresistance device because of its large magnetic g-factor (inversely proportional to the low

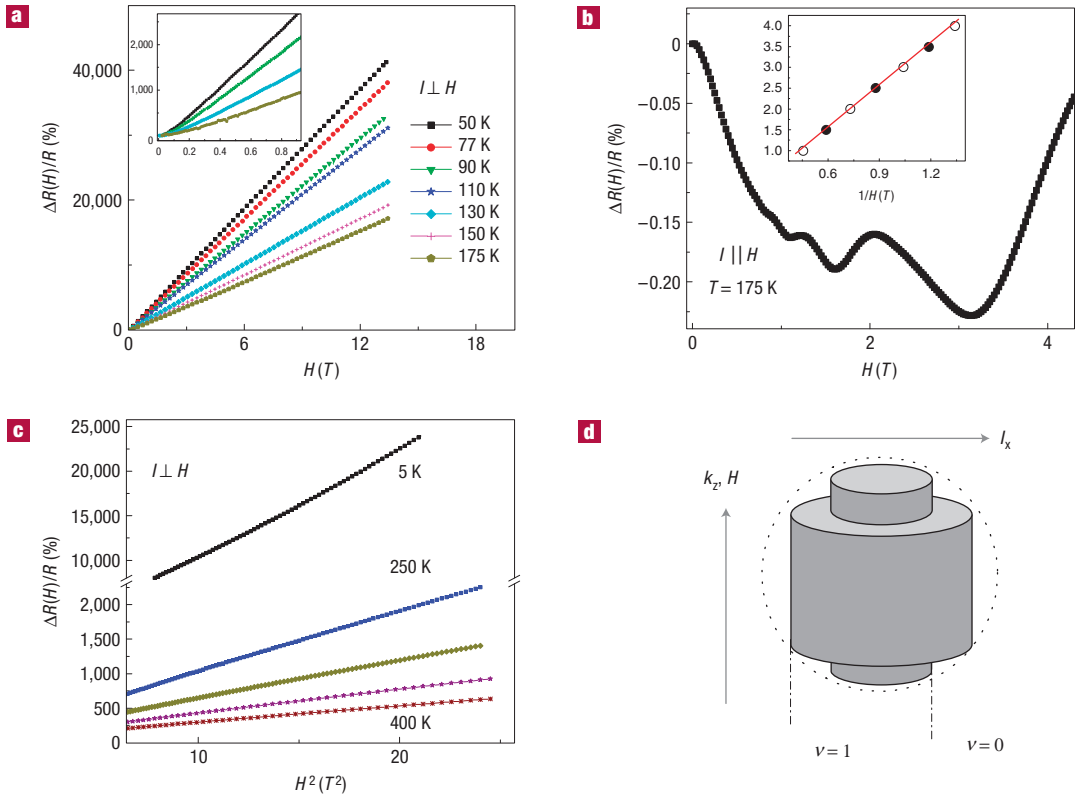

Figure 2 Linear quantum magnetoresistance of single-crystal InSb. a, The transverse magnetoresistance normalized to its zero-field value increases linearly with magnetic field in the extrinsic temperature regime. Inset: Low-field magnetoresistance at selected temperatures (50, 90, 130, 175 K) indicates a crossover to quadratic behaviour as $H \to 0$. **b**, The Shubnikov–de Haas oscillations observed in n-type InSb at $T = 175$ K in a longitudinal magnetic field establish the fundamental quantum nature of the transport. Inset: Filled (open) symbols correspond to peaks (valleys) of the oscillations. The solid line is a linear fit to $1/H$, characteristic of Landau-level physics. The material is in the extreme quantum limit for $H > 2$ T. **c**, The usual quadratic magnetic field dependence of the magnetoresistance characterizes the intrinsic regimes at low and high T. **d**, Schematic diagram of the 'extreme quantum limit', when only one or two Landau bands are filled. The levels $\nu = 0$ and 1 correspond to $H = 2$ and 1.2 T, respectively in **b**.

effective mass) and because the absolute value of the classical linear magnetoresistance, which can be directly related to the Hall voltage[5,7], tracks InSb's low electron concentration. Unlike the silver chalcogenides, however, InSb is known for its large, intrinsic magnetoresistance. Consequently, the presence of inhomogeneities leads to a linear magnetoresistance that will trump a quadratic magnetoresistance only at temperatures sufficiently high for the intrinsic magnetoresistance to be quenched by phonon scattering.

Figure 3b shows the normalized, transverse magnetoresistance of polycrystalline InSb, measured up to $H = 14$ T for $200\,\text{K} \leqslant T \leqslant 350\,\text{K}$ (above the quantum regime). The magnetoresistance of the inhomogeneous material is comparable to that of the pure crystal, and increases linearly with magnetic field, in agreement with the picture of inhomogeneous conductance. The fact that the magnetoresistance actually increases with T presumably reflects the dominance of the response by $\Delta\mu$. The disorder induced by non-stoichiometry transforms a narrow-gap semiconductor into a hybridized gapless state with a linear energy spectrum in both the valence and conduction bands[2]. The resulting band structure, shown in Fig. 3a, is analogous to that of single-layer graphite (graphene) in the vicinity of the Dirac point (differing only in dimensionality), where the predominant concentrations of electrons or holes are induced by positive/negative gate voltages[27,28]. The mobility fluctuations in our system are particularly acute when the gap goes to zero and both positive and negative values can be sampled[26], an effect that becomes increasingly more effective as temperature increases. For an inhomogeneous system, however, the averaged mobility cannot be simply obtained from a measurement of the Hall resistance. The experimental determination of the mobility distribution requires a more precise characterization of the internal structure. The Parish–Littlewood model simulates the inhomogeneity by randomly varying the mobility μ of an $N \times N$ resistor network, taking the distribution of μ to be Gaussian with average $\langle\mu\rangle$ and width $\Delta\mu$. Fits to the model yield $\langle\mu\rangle = 0$ and $\Delta\mu^{-1} = 0.5$ T, confirming that the observed crossover field is set by the width of the mobility fluctuations. The fact that the electrons and holes are present in equal proportions, as indicated by $\langle\mu\rangle = 0$, is consistent with the claim that the magnetoresistance is most linear when both positive and negative values of the mobility can be sampled.

The classical linear magnetoresistance observed in polycrystalline InSb is greatly surpassed by the quantum effects observed below 175 K, but it is favourable for wide-range field and current sensing in the high-T regime. The enhancement of the field sensitivity may not continue to increase greatly above $T = 400$ K given the observed trend in Fig. 3, but it should have considerable high-temperature head room given that InSb does not melt until 800 K. This hardy behaviour is in sharp contrast to homogeneous materials where rapidly decreasing carrier mobility with increasing T kills the magnetoresistance. It holds appeal for

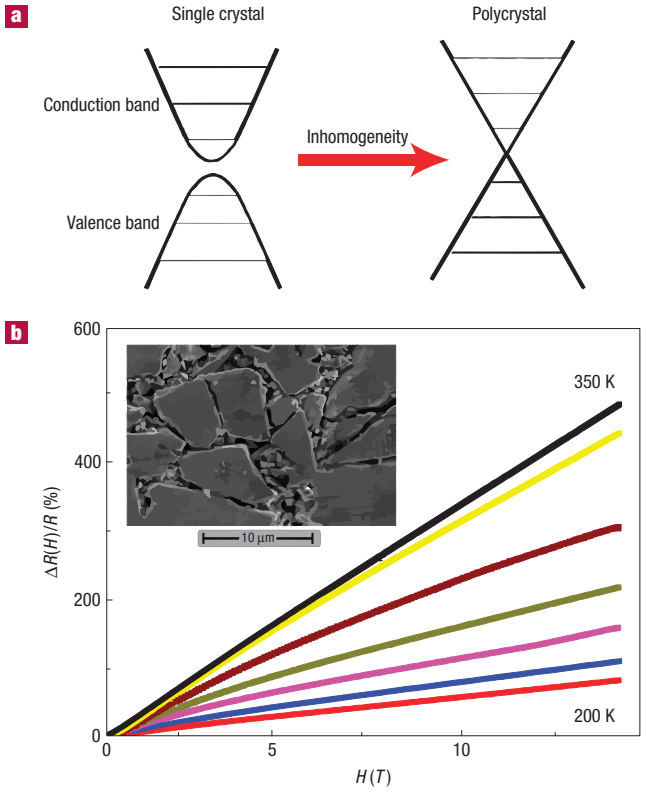

Figure 3 Linear classical magnetoresistance in macroscopically inhomogeneous InSb. a, Inhomogeneities create tails in both the conduction and valence bands and cause them to overlap. Mobility fluctuations are most acute near band crossing. **b**, The classical linear magnetoresistance dominates the intrinsic magnetoresistance (Fig. 2c) above room temperature. It actually increases with increasing T because of thermally aided mobility fluctuations. Inset: Scanning electron micrograph of an InSb polycrystal with typical grain size of 10–20 μm. The intergrain resistance can be estimated by comparing the zero-field resistivity of single-crystal and polycrystal InSb in their regimes of intrinsic conductivity (for example, at $T = 300$ K), where intrinsic carrier number and phonon scattering dominate the conductivity. We find the intergrain resistivity to be $9 \times 10^{-3}\,\Omega$ cm, approximately an order of magnitude higher than the resistivity of the pure crystal.

applications in ceramic engines for automobiles and aeroplanes, where magnetoresistive-based rotational speed gauges will need to operate at much higher temperatures than at present, as well as high field, non-saturating sensors for research at high T.

Moreover, devices with still higher inhomogeneous magnetoresistance are potentially achievable with artificially fabricated hybrid structures and conducting networks. A geometric technique has been implemented by Solin *et al.*[13] to massively enhance the low-field magnetoresistance of a composite InSb disc with metallic inclusions. Such an approach is promising for room-temperature magnetic sensors, but differs from the linear magnetoresistance in underlying mechanism (dependence on the intrinsic magnetoresistance of InSb), functional form (quadratic with field) and limiting field (saturating at $H \sim 5$ T). Graphene-based heterostructures also hold intriguing technological promise owing to their exceptionally large Hall coefficients and built-in gapless states. There is emerging evidence that the charge density in graphene field-effect transistors is mesoscopically inhomogeneous, and can be viewed as a chequerboard of n- and p-type doped regions separated by weakly conducting p–n junctions[29]. Interestingly, manipulation of current flows may be achieved by fine-tuning the density of carriers and gate voltages on both sides of the p–n junctions[30]. On these grounds, it could be anticipated that spatial variations of the effective gate voltage may induce pronounced mobility fluctuations and, consequently, a non-saturating linear magnetoresistance in a more controlled fashion.

Received 11 March 2008; accepted 21 July 2008; published 24 August 2008.

References

1. Abrikosov, A. A. Galvanomagnetic phenomena in metals in the quantum limit. *Sov. Phys.—JETP* **29**, 746–753 (1969).
2. Abrikosov, A. A. Quantum magnetoresistance. *Phys. Rev. B* **58**, 2788–2794 (1998).
3. Abrikosov, A. A. Quantum linear magnetoresistance. *Europhys. Lett.* **49**, 789–793 (2000).
4. Parish, M. M. & Littlewood, P. B. Non-saturating magnetoresistance in heavily disordered semiconductors. *Nature* **426**, 162–165 (2003).
5. Parish, M. M. & Littlewood, P. B. Classical magnetotransport of inhomogeneous conductors. *Phys. Rev. B* **72**, 094417 (2005).
6. Hu, J. S., Rosenbaum, T. F. & Betts, J. B. Current jets, disorder, and linear magnetoresistance in the silver chalcogenides. *Phys. Rev. Lett.* **95**, 186603 (2005).
7. Hu, J. S., Parish, M. M. & Rosenbaum, T. F. Nonsaturating magnetoresistance of inhomogeneous conductors: Comparison of experiment and simulation. *Phys. Rev. B* **75**, 214203 (2007).
8. Olsen, J. L. *Electron Transport in Metals* (Interscience, New York, 1962).
9. Binasch, G., Grünberg, P., Saurenbach, F. & Zinn, W. Enhanced magnetoresistance in layered magnetic structures with antiferromagnetic interlayer exchange. *Phys. Rev. B* **39**, 4828–4830 (1989).
10. Baibich, M. N. *et al.* Giant magnetoresistance of (001)Fe/(001)Cr magnetic superlattices. *Phys. Rev. Lett.* **61**, 2472–2475 (1988).
11. von Helmolt, R., Wecker, J., Holzapfel, B., Schultz, L. & Samwer, K. Giant negative magnetoresistance in perovskitelike $La_{2/3}Ba_{1/3}MnO_x$ ferromagnetic films. *Phys. Rev. Lett.* **71**, 2331–2333 (1993).
12. von Molnar, S., Briggs, A., Flouquet, J. & Remenyi, G. Electron localization in a magnetic semiconductor $Gd_{1-x}v_xS_4$. *Phys. Rev. Lett.* **51**, 706–709 (1983).
13. Solin, S. A. *et al.* Enhanced room-temperature geometric magnetoresistance in inhomogeneous narrow-gap semiconductors. *Science* **289**, 1530–1532 (2000).
14. Herring, C. Effect of random inhomogeneities on electrical and galvanomagnetic measurements. *J. Appl. Phys.* **31**, 1939–1953 (1960).
15. Kapitza, P. L. The study of the specific resistance of bismuth crystals and its change in strong magnetic fields and some allied problems. *Proc. R. Soc. London A* **119**, 358–443 (1928).
16. Yang, F. Y. *et al.* Large magnetoresistance of electrodeposited single-crystal bismuth thin films. *Science* **284**, 1335–1337 (1999).
17. Breckenridge, R. G. *et al.* Electrical and optical properties of intermetallic compounds I. Indium antimonide. *Phys. Rev.* **96**, 571–575 (1954).
18. Heremans, J. Solid-state magnetic field sensors and applications. *J. Phys. D* **26**, 1149–1168 (1993).
19. Hrostowski, H. J., Morin, F. J., Geballe, T. H. & Wheatley, G. H. Hall effect and conductivity of InSb. *Phys. Rev.* **100**, 1672–1676 (1955).
20. Madelung, O. *Physics of III–V Compounds* (Wiley, New York, 1964).
21. Fritzsche, H. & Lark-Horovitz, K. Electrical properties of *p*-type indium antimonide at low temperatures. *Phys. Rev.* **99**, 400–405 (1955).
22. Frederikse, H. P. R. & Hosler, W. R. Galvanomagnetic effects in *n*-type indium antimonide. *Phys. Rev.* **108**, 1136–1145 (1957).
23. Xu, R. *et al.* Large magnetoresistance in non-magnetic silver chalcogenides. *Nature* **390**, 57–60 (1997).
24. Ogorelec, Z., Hamzic, A. & Basletic, M. On the optimization of the large magnetoresistance of Ag_2Se. *Europhys. Lett.* **46**, 56–61 (1999).
25. Husmann, A. *et al.* MegaGauss sensors. *Nature* **417**, 421–424 (2002).
26. Lee, M., Rosenbaum, T. F., Saboungi, M.-L. & Schnyders, H. S. Band-gap tuning and linear magnetoresistance in silver chalcogenides. *Phys. Rev. Lett.* **88**, 066602 (2002).
27. Novoselov, K. S. *et al.* Electric field effect in atomically thin carbon films. *Science* **306**, 666–669 (2004).
28. Novoselov, K. S. *et al.* Two-dimensional gas of massless Dirac fermions in graphene. *Nature* **438**, 197–200 (2005).
29. Cheianov, V. V. *et al.* Random resistor network model of minimal conductivity in graphene. *Phys. Rev. Lett.* **99**, 176801 (2007).
30. Cheianov, V. V., Fal'ko, V. & Altshuler, B. L. The focusing of electron flow and a Veselago lens in graphene. *Science* **315**, 1252–1255 (2007).

Acknowledgements

The authors thank M. M. Parish for valuable discussions on the Parish–Littlewood model. The work at the University of Chicago was supported by DOE Basic Energy Sciences.

Author contributions

J.H. and T.F.R. contributed equally to all parts of the project.

Author information

Reprints and permission information is available online at http://npg.nature.com/reprintsandpermissions. Correspondence and requests for materials should be addressed to T.F.R.